Inorg. Chem. **2006**, *45*, 4769–4782

Fast Catalytic Hydroxylation of Hydrocarbons with Ruthenium Porphyrins

Chuanqing Wang, Kirill V. Shalyaev, Marcella Bonchio, Tommaso Carofiglio, and John T. Groves*

Department of Chemistry, Princeton University, Princeton, New Jersey 08544

Received November 30, 2005

Ruthenium porphyrin complexes such as carbonylruthenium(II) tetrakispentafluorophenylporphyrin [Ru^{II}(TPFPP)(CO)] were found to be efficient catalysts for the hydroxylation of alkanes in the presence of 2,6-dichloropyridine *N*-oxide as the oxidant under mild, nonacidic conditions. Up to 14 800 turnovers (TO) and rates of 800 TO/min were obtained for the hydroxylation of adamantane. The hydroxylation of *cis*-decalin afforded *cis*-9-decalol and *cis*-decalin-9,10-diol, exclusively, thus, excluding a long-lived radicals mechanism. The kinetics of product evolution in a typical catalytic oxygenation showed an initial induction period followed by a fast, apparently zero-order phase with maximum rates and high efficiencies. Deuterium isotope effects (k_H/k_D) in the range of 4.2–6.4 were found for the hydroxylation of alkanes. A Hammett treatment of the data for the oxidation of para-substituted toluene derivatives showed a linear correlation with a highly negative ρ^+ value of –2.0. On the basis of kinetic and spectroscopic evidence, Ru^{VI}(TPFPP)$(O)_2$, Ru^{II}(TPFPP)(CO), and Ru^{IV}(TPFPP)Cl_2 observed during catalysis were ruled out as candidates for the active catalyst responsible for the high efficiencies and turnover rates in the oxidation reactions. The fastest rates of adamantane hydroxylation with 2,6-dichloropyridine *N*-oxide were achieved by the reductive activation of Ru^{IV}(TPFPP)Cl_2 with a zinc amalgam. This redox activation is consistent with the formation of an active Ru(III) intermediate in situ by a one-electron reduction of the Ru(IV) porphyrin. EPR spectra characteristic of Ru(III) have been observed upon the reduction of Ru^{IV}(TPFPP)Cl_2 with a zinc amalgam. In the adamantane oxidation mediated with Ru^{III}(TPFPP)(OEt), it was found that, during this process, the Ru(III) porphyrin was gradually converted to a dioxoRu(VI) porphyrin. Concomitant with this conversion, the reaction rates decreased. Catalyst activation was also stimulated by autoxidation of the solvent CH_2Cl_2. On the basis of these data, a mechanism is proposed that incorporates a "fast" cycle involving metastable Ru(III) and oxoRu(V) intermediates and a "slow" oxidation cycle, mediated by oxoRu(IV) and *trans*-dioxoRu(VI) porphyrin complexes.

Introduction

Nature selected iron porphyrins to mediate intrinsically difficult oxidations with dioxygen at the heme center of cytochrome P450 monooxygenases.[1−4] An extensive variety of cytochrome P450 models has been developed over the past three decades and applied to hydrocarbon oxidations with the aims of both developing useful catalysts and probing the mechanisms of these processes. Ruthenium porphyrins and related complexes have received considerable attention because of the close periodic relationship to the biologically significant iron and the rich coordination and redox chemistry of ruthenium, which spans oxidation states from +2 to +7 in the porphyrin ligand environment.[5−17]

* Author to whom correspondence should be addressed. Phone: (609) 258-3593. Fax: (609) 258-0348. E-mail: jtgroves@princeton.edu.

(1) Groves, J. T. In *Cytochrome P450: Structure, Mechanism, and Biochemistry*, 3rd ed.; Ortiz de Montellano, P. R., Ed.; Klewer Academic/Plenum: New York, 2004; pp 1−44.
(2) Groves, J. T. *Proc. Natl. Acad. Sci. U.S.A.* **2003**, *100*, 3569−3574.
(3) He, X.; Cryle, M. J.; DeVoss, J. J.; de Montellano, P. R. O. *Drug Metab. Rev.* **2004**, *36*, 6.
(4) Meunier, B.; de Visser, S. P.; Shaik, S. *Chem. Rev.* **2004**, *104*, 3947−3980.
(5) Griffith, W. P. *Chem. Soc. Rev.* **1992**, *21*, 179−185.
(6) Mlodnicka, T.; James, B. R.; Montanari, F.; Casella, L. *Metalloporphyrins Catalyzed Oxidations*; Kluwer Academic Publishers: Netherlands, 1994.
(7) Ito, R.; Umezawa, N.; Higuchi, T. *J. Am. Chem. Soc.* **2005**, *127*, 834−835.
(8) Jitsukawa, K.; Oka, Y.; Yamaguchi, S.; Masuda, H. *Inorg. Chem.* **2004**, *43*, 8119−8129.
(9) Chen, J.; Che, C. M. *Angew. Chem., Int. Ed.* **2004**, *43*, 4950−4954.
(10) Chatterjee, D.; Mitra, A.; Shepherd, R. E. *Inorg. Chim. Acta* **2004**, *357*, 980−990.
(11) Le Maux, P.; Lukas, M.; Simonneaux, G. *J. Mol. Catal. A* **2003**, *206*, 95−103.
(12) Berkessel, A.; Kaiser, P.; Lex, J. *Chem.—Eur. J.* **2003**, *9*, 4746−4756.

10.1021/ic0520566 CCC: $33.50
Published on Web 05/18/2006

Notably, ruthenium porphyrins have been shown to utilize dioxygen in air for the clean epoxidation of olefins under mild conditions,[18] and they have also shown promise in the activation of nitrous oxide.[19−23] The mechanism of aerobic epoxidation mediated by ruthenium porphyrins has been examined, and a *trans*-dioxoruthenium(VI) complex was found to be the active oxidant. Unfortunately, these reactions afforded only ca. 50 turnovers (TO) and proceeded at relatively slow rates of 1−2 turnovers per hour. Hirobe et al. have reported the use of 2,6-disubstituted pyridine *N*-oxides as oxygen donors with ruthenium porphyrins such as Ru^{II}(TMP)(CO) and Ru^{VI}(TMP)$(O)_2$. High turnover numbers on the order of 10 000 were reported for this system.[24−26] We have reported on the high activity of ruthenium pentafluorophenyl porphyrins in similar oxidations.[27,28] These studies have suggested that an active oxidant other than the previously characterized *trans*-dioxoruthenium(VI) may be responsible for these highly efficient oxygenations with 2,6-disubstituted pyridine *N*-oxides,[29,30] but the mechanism and the nature of the active oxidant species in this system has remained unclear.

Here, we report our full findings on the mechanism of hydrocarbon hydroxylation mediated by polyhalogenated ruthenium porphyrin catalysts with 2,6-dichloropyridine *N*-oxide as the oxidant. Remarkable rates, selectivities, and efficiencies have been achieved for the catalytic oxygenations with polyhalogenated ruthenium porphyrins. We show that the Ru(II), Ru(IV), and Ru(VI) porphyrin species observed during catalysis act as a reservoir of catalyst precursors, each with marginal activity. The results support a Ru(III)−oxoRu(V) cycle for the "fast catalysis" as we have previously suggested.[27,28]

Scheme 1. Hydroxylation of Hydrocarbons with 2,6-Dichloropyridine *N*-Oxide Catalyzed by Ru^{II}(TPFPP)(CO)

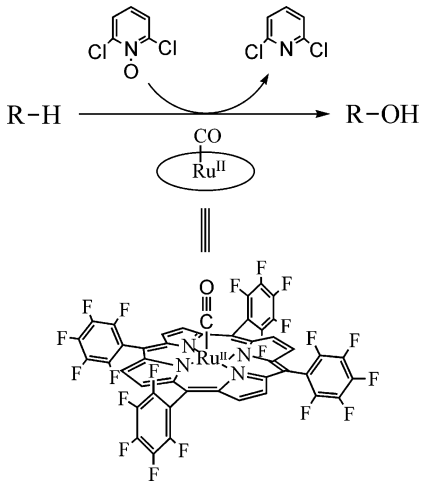

Results and Discussion

Scope of Oxidative Catalysis by Ruthenium Porphyrins. Ruthenium porphyrin complexes such as carbonylruthenium(II) tetrakispentafluorophenylporphyrin [Ru^{II}(TPFPP)(CO)] efficiently catalyzed the hydroxylation of unactivated alkanes, the cleavage of ethers, and the oxygenation of benzene with 2,6-dichloropyridine *N*-oxide as the oxidant under mild, nonacidic conditions (Scheme 1). The hydroxylation of adamantane proceeded with turnover rates up to 800 TO/min at high *N*-oxide concentrations and gave 14 800 catalytic turnovers. Up to 3100 turnovers at the maximum rate of 30 TO/min have been obtained in the hydroxylation of cyclohexane mediated by Ru^{II}(TPFPP)(CO). In a similar reaction, benzene was oxidized to benzoquinone (Table 1).

Maximum turnover numbers that we obtained for the hydroxylation of cyclohexane were compared with carbonylruthenium(II) tetramesitylylporphyrin [Ru^{II}(TMP)(CO)] and two pentafluorophenyl ruthenium porphyrin catalysts, Ru^{II}(TPFPP)(CO) and the β-pyrrole octabrominated analogue Ru^{II}(TPFPPBr_8)(CO). Ultimately, the ruthenium porphyrins were completely degraded, as evidenced by the decrease of their Soret absorbances in the UV−vis spectra and a loss of catalytic activity. Catalyst stability dramatically improved with increased halogenation of the porphyrin macrocycles. Polyhalogenated ruthenium porphyrins are known to have enhanced stability toward oxidative degradation.[31,32] In typical runs, Ru^{II}(TMP)(CO) gave 300 TO, and Ru^{II}(TPFPP)(CO) afforded 2500 TO. The greatest number of turnovers for cyclohexane oxidation, nearly 6000, was achieved with completely halogenated Ru^{II}(TPFPPBr_8)(CO).

Hydroxylations with polyhalogenated ruthenium porphyrins were characterized by extraordinary selectivity. For example, the 3°/2° preference on a per hydrogen basis for the Ru^{II}(TPFPP)(CO)-catalyzed oxidation of adamantane was nearly 200. By comparison, tertiary versus secondary C−H selectivities are reported to be 11−48 for iron porphyrin

(13) Zhang, R.; Yu, W. Y.; Sun, H. Z.; Liu, W. S.; Che, C. M. *Chem.—Eur. J.* **2002**, *8*, 2495−2507.
(14) Bonchio, M.; Scorrano, G.; Toniolo, P.; Proust, A.; Artero, V.; Conte, V. *Adv. Synth. Catal.* **2002**, *344*, 841−844.
(15) Zhang, R.; Yu, W. Y.; Wong, K. Y.; Che, C. M. *J. Org. Chem.* **2001**, *66*, 8145−8153.
(16) Nakata, K.; Takeda, T.; Mihara, J.; Hamada, T.; Irie, R.; Katsuki, T. *Chem.—Eur. J.* **2001**, *7*, 3776−3782.
(17) Ogliaro, F.; de Visser, S. P.; Groves, J. T.; Shaik, S. *Angew. Chem., Int. Ed.* **2001**, *40*, 2874−2878.
(18) Groves, J. T.; Quinn, R. *J. Am. Chem. Soc.* **1985**, *107*, 5790−5792.
(19) Groves, J. T.; Roman, J. S. *J. Am. Chem. Soc.* **1995**, *117*, 5594−5595.
(20) Tanaka, H.; Hashimoto, K.; Suzuki, K.; Kitaichi, Y.; Sato, M.; Ikeno, T.; Yamada, T. *Bull. Chem. Soc. Jpn.* **2004**, *77*, 1905−1914.
(21) Hashimoto, K.; Tanaka, H.; Ikeno, T.; Yamada, T. *Chem. Lett.* **2002**, 582−583.
(22) Ben-Daniel, R.; Weiner, L.; Neumann, R. *J. Am. Chem. Soc.* **2002**, *124*, 8788−8789.
(23) Yamada, T.; Hashimoto, K.; Kitaichi, Y.; Suzuki, K.; Ikeno, T. *Chem. Lett.* **2001**, 268−269.
(24) Ohtake, H.; Higuchi, T.; Hirobe, M. *Heterocycles* **1995**, *40*, 867−903.
(25) Higuchi, T.; Hirobe, M. *J. Mol. Catal. A* **1996**, *113*, 403−422.
(26) (a) Shingaki, T.; Miura, K.; Higuchi, T.; Hirobe, M.; Nagano, T. *Chem. Commun.* **1997**, 861−862. (b) Higuchi, T.; Ohtake, H.; Hirobe, M. *Tetrahedron Lett.* **1989**, *30*, 6545−6548.
(27) Groves, J. T.; Bonchio, M.; Carofiglio, T.; Shalyaev, K. *J. Am. Chem. Soc.* **1996**, *118*, 8961−8962.
(28) Groves, J. T.; Shalyaev, K. V.; Bonchio, M.; Carofiglio, T. *Stud. Surf. Sci. Catal.* **1997**, *110*, 865−872.
(29) Zhang, J. L.; Che, C. M. *Chem.—Eur. J.* **2005**, *11*, 3899−3914.
(30) Ogawa, S.; Iida, T.; Goto, T.; Mano, N.; Goto, J.; Nambara, T. *Org. Biomol. Chem.* **2004**, *2*, 1013−1018.
(31) Traylor, P. S.; Dolphin, D.; Traylor, T. G. *J. Chem. Soc., Chem. Commun.* **1984**, 279−280.
(32) Wijesekera, T. P.; Lyons, J. E.; Ellis, P. E. *Catal. Lett.* **1996**, *36*, 69−73.

Table 1. Oxidations with 2,6-Dichloropyridine *N*-Oxide Catalyzed by Ru(TPFPP) Complexes[a]

number	substrate, M	*N*-oxide, M	time, min	product, (yield[b], %)	TO[c] (max. rate, TO/min)
1	*cis*-decalin, 0.02	0.02	25	*cis*-9-decalol (80)	320 (64)
				cis-decalin-9,10-diol (8.4)	34
2	2,2,3-trimethylbutane, 0.04	0.02	100	2,3,3-trimethyl-2-butanol (88)	352
3	adamantane, 0.2[d]	0.2	120	1-adamantanol (61)	12070 (800)
				adamantane-1,3-diol (6.0)	1180
				2-adamantanol (0.59)	87
				2-adamantanone (0.97)	142
4	cyclohexane, 2.0[d]	0.05	100	cyclohexanol (49)	1080 (30)[e]
				cyclohexanone (35)	376
5	cyclohexane, 2.0[d,f] (CH_2Cl_2/CCl_3Br 80:20%)	0.05	20 h	cyclohexanol (18)	154[e]
				cyclohexanone (55)	232
				bromocyclohexane (0.9)	7.5
6	toluene, 0.2	0.02	90	benzoic acid (61)	82
				benzyl alcohol (9.3)	37
				benzaldehyde (7.2)	15
				benzyl chloride (1.6)	6
7	benzene, 2.0	0.02	12 h	1,4-benzoquinone (40)	53[e]
8	dibutyl ether, 0.2	0.02	180	butyraldehyde (80)	320
				1-butanol (92)	368
9	cyclohexyl acetate, 0.1	0.05	250	3-acetoxycyclohexanone (33)	165
				4-acetoxycyclohexanone (42)	210
				cyclohexanone (1.5)	15
10	cyclopentyl acetate, 0.1	0.05	200	3-acetoxycyclopentanone (61)	158
11	cyclohexanol, 0.04[g]	0.02	240	cyclohexanone (85)	268 (1.2)[e]
12	cyclobutanol, 0.04	0.02	14 h	cyclobutanone (60)	76[e]

[a] Catalyst, Ru^{II}(TPFPP)(CO); [cat.] = 5×10^{-5} M; CH_2Cl_2; 65 °C. [b] Percent yield based on oxidant consumed. [c] Turnover number, TO = [product]/[catalyst]. [d] [Ru^{II}(TPFPP)(CO)] = 1×10^{-5} M. [e] The reaction was stopped before consumption of the *N*-oxide. [f] Reaction was carried out at 25 °C. [g] Catalyst, Ru^{VI}(TPFPP)$(O)_2$; [cat.] = 5×10^{-5} M; 40 °C.

catalyzed hydroxylations,[33] 3−10 for manganese porphyrin mediated oxidations,[34] 10 for reactions of the *tert*-butoxy radical,[35] and about 2 for the oxidation of alkanes by hydroxyl radicals.[36] The oxidation of *cis*-decalin was completely stereospecific with *cis*-9-decalol and *cis*-decalin-9,-10-diol produced in high yields (90%; Table 1). No *trans*-9-decalol was detected. Likewise, *trans*-decalin gave *trans*-9-decalol and no *cis*-9-decalol, as we have reported.[27] Similar selectivity has been reported by Hirobe et al. in a related system[24] and recently by Bonchio et al. for ruthenium oxometalates.[14]

Remarkably, the oxidation of cyclohexyl acetate with Ru^{II}-(TPFPP)(CO)/2,6-dichloropyridine *N*-oxide gave a mixture of 3- and 4-acetoxycyclohexanones (75% combined yield based on the oxidant consumed). Only a trace of cyclohexanone was produced, and no 2-acetoxycyclohexanone was detected. A single ketone, 3-acetoxycyclopentanone, was formed in cyclopentyl acetate oxidation. For both substrates, the acetyl group provided complete protection against oxidation of the C−H bonds in the α and β positions relative to the acetate group.

Catalytic oxygenation of dibutyl ether resulted in clean cleavage to give 1-butanol and butyraldehyde in high yields. Cyclohexanol was selectively oxidized to cyclohexanone.

Reaction Kinetics. These catalytic oxygenation reactions have been found to follow an unusual time course. Typical kinetic profiles for adamantane hydroxylation with 2,6-dichloropyridine *N*-oxide catalyzed by Ru^{II}(TPFPP)(CO) or Ru^{VI}(TPFPP)$(O)_2$ showed an induction period followed by a linear, apparently zero-order phase, as we have reported (Figure 1).[27] This linear phase of the product appearance profile extended until ca. 80% of the oxidant and substrate had been consumed. Significantly, the starting catalyst, Ru^{II}-(TPFPP)(CO) or Ru^{VI}(TPFPP)$(O)_2$, remained the major ruthenium porphyrin species present during ca. 400 turnovers of adamantane hydroxylation, as revealed by the UV−vis monitoring of the two reactions during turnover.

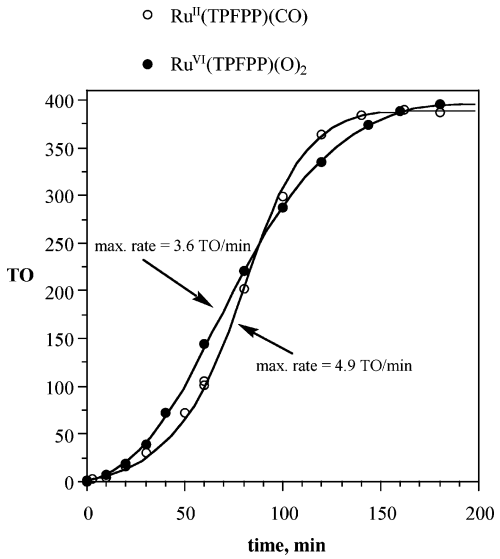

Figure 1. Kinetics of adamantane hydroxylation with 2,6-dichloropyridine *N*-oxide catalyzed by Ru^{VI}(TPFPP)$(O)_2$ and Ru^{II}(TPFPP)(CO). [adamantane] = 0.02 M, [RuPor] = 50 μM, [2,6-dichloropyridine *N*-oxide] = 0.02 M; 40 °C.

The catalytic hydroxylation of cyclohexane, which is a less active substrate than adamantane, also proceeded with

(33) Groves, J. T.; Nemo, T. E. *J. Am. Chem. Soc.* **1983**, *105*, 6243−6248.
(34) Hoffmann, P.; Robert, A.; Meunier, B. *Bull. Soc. Chim. Fr.* **1992**, *129*, 85−97.
(35) Barton, D. H. R.; Hu, B.; Taylor, D. K.; Wahl, R. U. R. *J. Chem. Soc., Perkin Trans. 2* **1996**, 1031−1041.
(36) Russell, G. A. In *Free Radicals*; Kochi, J., Ed.; Wiley-Interscience: New York, 1973; Vol. II, pp 689−690.

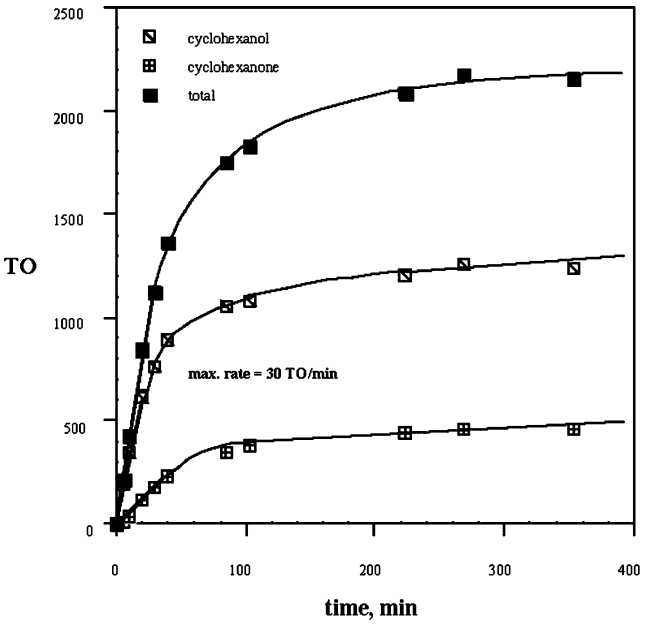

Figure 2. Kinetics of cyclohexane hydroxylation with 2,6-dichloropyridine *N*-oxide catalyzed by Ru^{II}(TPFPP)(CO). [cyclohexane] = 2.0 M, [Ru^{II}(TPFPP)(CO)] = 10 μM, [2,6-dichloropyridine *N*-oxide] = 0.05 M; CH_2Cl_2; 65 °C.

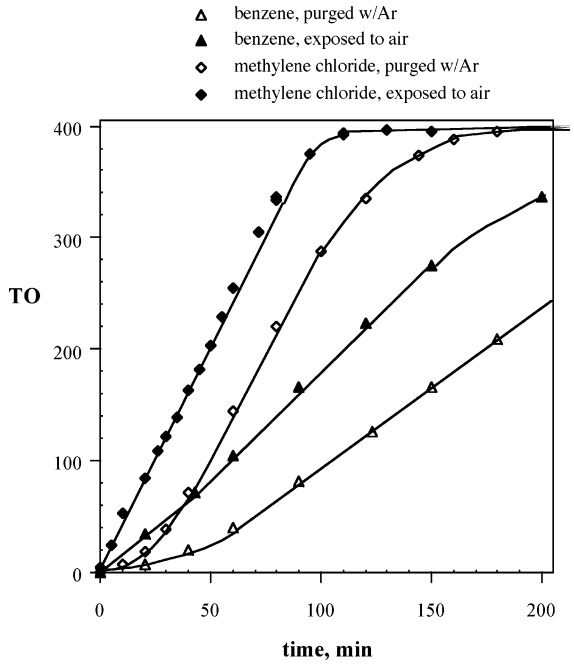

Figure 3. Effect of dioxygen on the induction period of adamantane hydroxylation with 2,6-dichloropyridine *N*-oxide catalyzed by Ru^{VI}(TPFPP)$(O)_2$. [adamantane] = 0.02 M, [Ru^{VI}(TPFPP)$(O)_2$] = 50 μM, [2,6-dichloropyridine *N*-oxide] = 0.02 M; 40 °C.

a fast initial linear phase (30 TO/min maximum rate at 65 °C) but eventually slowed because of the oxidative destruction of the porphyrin catalyst (bleaching) as revealed by the decrease in the UV−vis absorbance (λ_{max} = 402 nm) in the Soret region of Ru^{II}(TPFPP)(CO) (Figure 2). Both cyclohexanol and cyclohexanone were formed (Table 1, entries 4 and 5). The relative reactivity of cyclohexane and cyclohexanol, determined from the kinetics of the product evolution, remained constant throughout the entire course of the reaction ($k_{cyclohexanol}/k_{cyclohexane}$ = 123 ± 5, see Experimental Section). This observation is consistent with a sequential oxidation to cyclohexanol and then cyclohexanone.

The induction period for the catalytic oxidations mediated by Ru^{II}(TPFPP)(CO) and Ru^{VI}(TPFPP)$(O)_2$ was shortened with an increase in the reaction temperature and by exposure to visible light.[27] Interestingly, there was a distinct effect of air on the kinetic profiles of the product evolution. The kinetics of adamantane hydroxylation with Ru^{VI}(TPFPP)$(O)_2$/2,6-dichloropyridine *N*-oxide in methylene chloride showed no detectable induction period when air was not strictly excluded from the reaction medium (Figure 3). The presence of air in the reaction system slightly increased the maximum rates of adamantane hydroxylation, measured as the slope of the linear phase of kinetic traces (Table 2, entries 8−11; also see Figure 3).

We found that acids suppressed the rates of oxidations mediated by Ru(TPFPP) complexes. When anhydrous HCl was introduced to the reaction mixture of adamantane hydroxylation in the presence of Ru^{VI}(TPFPP)$(O)_2$, the rate of the catalytic oxidation decreased 8-fold (Table 2, entries 11 and 12). Trifluoroacetic acid produced a similar inhibiting effect. By contrast, the addition of mineral acids such as HCl and HBr was essential for the hydroxylation of alkanes in the catalytic system of Hirobe et al. in which Ru(TPP) and Ru(TMP) catalysts were used.[24,25]

The rates of catalytic hydroxylations were highly temperature-dependent. A linear Eyring plot was obtained for the rate of adamantane hydroxylation with a Ru^{VI}(TPFPP)$(O)_2$ catalyst (Figure 4) with an apparent enthalpy of activation $\Delta H^{\ddagger}$ = 19 kcal/mol (R = 0.994).

The Role of Ru^{VI}(TPFPP)$(O)_2$ in the Catalysis of Alkane Hydroxylation. The similarity of the turnover rates and small changes in the visible spectra during reactions with Ru^{II}(TPFPP)(CO) and Ru^{VI}(TPFPP)$(O)_2$ indicate that neither Ru^{II}(TPFPP)(CO) nor Ru^{VI}(TPFPP)$(O)_2$ lie on the "fast" catalytic oxidation pathway. Obviously, Ru^{II}(TPFPP)(CO) cannot be directly involved in the catalytic cycle and would need to be activated in some way. The fact that the *trans*-dioxoRu(VI) trace for adamantane hydroxylation has an induction period also argues against *trans*-dioxoRu(VI) being the only active species. The induction period implies that, as in the case of Ru^{II}(TPFPP)(CO), the *trans*-dioxoRu(VI) catalyst also undergoes activation before the maximum turnover rates can be reached.

We have quantitatively evaluated the role of *trans*-dioxoRu(VI) porphyrins in the fast catalysis process by examining the stoichiometric reactions of these species. We found that one equivalent of Ru^{VI}(TPFPP)$(O)_2$ oxidized the tertiary C−H positions of *cis*-decalin to produce one equivalent of *cis*-9-decalol in nearly quantitative yield (99%; Scheme 2). The reaction was completely stereospecific, and no *trans*-9-decalol or secondary C−H bond oxidation products were detected. The porphyrin product, which was isolated from the reaction mixture in high yield, had a diamagnetic NMR resonance at δ 8.62 for the pyrrole protons and displayed an intense cluster of peaks at m/z = 2164 in the FAB−MS spectrum, which corresponds to the mass of a dimeric [Ru(TPFPP)]$_2$O fragment. Considered together with

Table 2. Hydroxylation of Adamantane with 2,6-Dichloropyridine *N*-Oxide Catalyzed by Ru(TPFPP) Complexes[a]

number	catalyst	solvent	time, min	*T*, °C	atmosphere[b]	TON	max. rate, TO/min
1	$Ru^{IV}(TPFPP)Cl_2$ + Zn(Hg)	CH_2Cl_2	50	25	Ar	380	31.4
2	$Ru^{IV}(TPFPP)Cl_2$	CH_2Cl_2	208	25	Ar	336	6.3
3	$Ru^{IV}(TPFPP)Cl_2$	CH_2Cl_2	50	25	air	309	11.5
4	$Ru^{IV}(TPFPP)Cl_2$	$PhCF_3$	50	25	Ar	105	4.6
5	$Ru^{IV}(TPFPP)Cl_2$	$PhCF_3$	45	25	air	112	5.1
6	$Ru^{II}(TPFPP)(CO)$	CH_2Cl_2	753	25	air	275	0.43
7	$Ru^{VI}(TPFPP)(O)_2$	CH_2Cl_2	190	25	air	74	0.39
8	$Ru^{VI}(TPFPP)(O)_2$	CH_2Cl_2	180	40	Ar	395	3.6
9	$Ru^{VI}(TPFPP)(O)_2$	CH_2Cl_2	150	40	air	395	4.1
10	$Ru^{VI}(TPFPP)(O)_2$	C_6H_6	200	40	Ar	209	1.4
11	$Ru^{VI}(TPFPP)(O)_2$	C_6H_6	270	40	air	359	1.9
12	$Ru^{VI}(TPFPP)(O)_2$	C_6H_6, HCl[c]	200	40	air	57	0.25
13	$Ru^{II}(TPFPP)(CO)$	CH_2Cl_2	20	65	air	364	72

[a] [Adamantane] = [2,6-dichloropyridine *N*-oxide] = 0.02 M; [catalyst] = 5×10^{-5} M. Yields of 1-adamantanol and 1,3-adamantanediol were 91−97% based on oxidant consumed. [b] Reaction conditions: Ar, reaction was conducted under argon. [c] A total of 20 μL of saturated HCl (anh.) solution in benzene was added to a 2 mL sample.

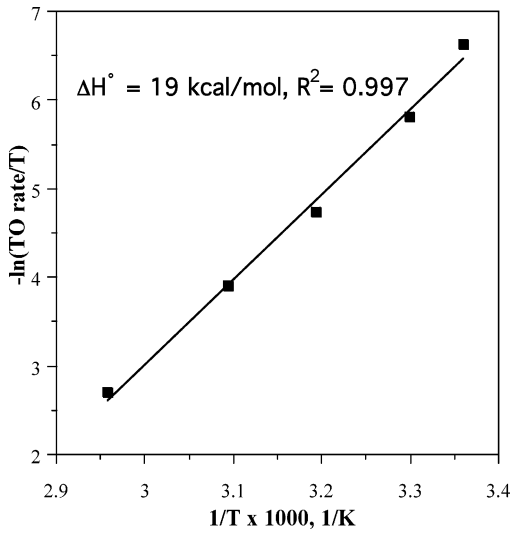

Figure 4. Eyring plot for adamantane hydroxylation with 2,6-dichloropyridine *N*-oxide catalyzed by $Ru^{VI}(TPFPP)(O)_2$. [adamantane] = 0.02 M, [$Ru^{VI}(TPFPP)(O)_2$] = 50 μM, [2,6-dichloropyridine *N*-oxide] = 0.02 M; CH_2Cl_2; 40 °C.

Scheme 2. Stoichiometric Hydroxylation of *cis*-Decalin with $Ru^{VI}(TPFPP)(O)_2$

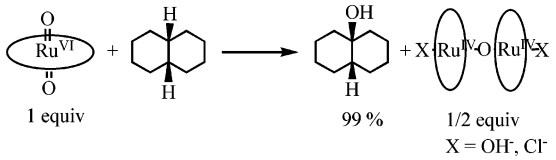

the stoichiometry of *cis*-decalin oxidation, these data support the assignment of this diamagnetic porphyrin as a μ-oxoruthenium(IV) dimer.[37−41] We found that such a μ-oxo dimer could also be produced by the slow (72 h) decomposition of $Ru^{VI}(TPFPP)(O)_2$ in methylene chloride in the absence of a substrate.

trans-DioxoRu(VI) complexes have been shown to be the active species in epoxidations catalyzed by ruthenium complexes.[18,42] Che et al.[37] have demonstrated that, in addition to being reactive toward alkenes, *trans*-dioxoRu(VI) porphyrins, $Ru^{VI}(TPP)(O)_2$ and $Ru^{VI}(OEP)(O)_2$, were selective oxidants for the tertiary C−H bonds of alkanes. However, the stoichiometric reactions of these ruthenium porphyrin complexes with alkanes proceeded with low efficiency because the rate of oxidation was too slow to compete with the self-degradation of the ruthenium complexes. For example, only ∼20% yields of 1-adamantanol were obtained in the oxidation of adamantane.

A comparison of the rates of the stoichiometric hydrocarbon oxidations by $Ru^{VI}(TPFPP)(O)_2$ with those of the catalytic oxidations with 2,6-dichloropyridine *N*-oxide showed that the catalytic reactions were too fast to be due to the reaction of $Ru^{VI}(TPFPP)(O)_2$. The rates of the stoichiometric reactions of $Ru^{VI}(TPFPP)(O)_2$ with several substrates were measured in two ways: by monitoring the disappearance of UV−vis absorbance of the Ru(VI) porphyrin or by following the intensity of the pyrrole proton resonance of the *trans*-dioxoRu(VI) complex at δ 9.26 in ^{1}H NMR spectra. The reactions were carried out under pseudo-first-order conditions with excess substrate relative to the ruthenium porphyrin. The second-order rate constants of the stoichiometric oxidations (k_{st}) determined from a single-exponential fit of the data to eq 1 are shown in Table 3.

$$\text{Rate} = -\text{d}[Ru^{VI}(TPFPP)(O)_2]/\text{d}t = k_{st}[\text{substrate}][Ru^{VI}(TPFPP)(O)_2] \quad (1)$$

Turnover rates for the catalytic reactions were measured as the slope of the linear phase of kinetic traces of product evolution in hydrocarbon oxidations with 2,6-dichloropyridine *N*-oxide as an oxygen donor in the presence of $Ru^{VI}(TPFPP)(O)_2$. We estimated the catalytic rate constants (k_{cat}) assuming that the *trans*-dioxoRu(VI) porphyrin is the sole active catalytic species, and it is the reaction of this dioxoRu(VI) species with the substrate that determines the turnover

(37) Ho, C.; Leung, W. H.; Che, C. M. *J. Chem. Soc., Dalton Trans.* **1991**, 2933−2939.
(38) Collman, J. P.; Barnes, C. E.; Brothers, P. J.; Collins, T. J.; Ozawa, T.; Gallucci, J. C.; Ibers, J. A. *J. Am. Chem. Soc.* **1984**, *106*, 5151−5163.
(39) Leung, W. H.; Che, C. M. *J. Am. Chem. Soc.* **1989**, *111*, 8812−8818.
(40) Masuda, H.; Taga, T.; Osaki, K.; Sugimoto, H.; Mori, M.; Ogoshi, H. *J. Am. Chem. Soc.* **1981**, *103*, 2199−2203.
(41) Sugimoto, H.; Higashi, T.; Mori, M.; Nagano, M.; Yoshida, Z.; Ogoshi, H. *Bull. Chem. Soc. Jpn.* **1982**, *55*, 822−828.
(42) Rajapakse, N.; James, B. R.; Dolphin, D. *Catal. Lett.* **1989**, *2*, 219−225.

Table 3. Comparison of Actual Rate Constants for Stoichiometric $Ru^{VI}(TPFPP)(O)_2$ Reactions with Minimum, Hypothetical Rate Constants for Catalytic Reactions of $Ru^{VI}(TPFPP)(O)_2$

substrate	*T*, °C	stoichiometric oxidation k_{st}, M^{-1} s^{-1}, (R)	catalytic oxidation k_{cat},[a] M^{-1} s^{-1}, (R)	major resting state of the catalyst[b]	k_{cat}/k_{st} [a]
cis-decalin	25	2.3×10^{-3} (0.978)	1.9×10^{-2} [0.38] (0.990)	$Ru^{VI}(TPFPP)(O)_2$	8.3 [165]
adamantane	40	3.1×10^{-1} (0.998)	3.0 [60] (0.999)	$Ru^{VI}(TPFPP)(O)_2$	9.7 [194]
benzyl alcohol	40	6.0×10^{-2} (0.999)	2.8 [56] (0.989)	$Ru^{VI}(TPFPP)(O)_2$	46.6 [933]
cyclohexanol	40	1.5×10^{-3} (0.999)	5.0×10^{-1} [10] (0.999)	N/D	330 [6.6×10^3]
styrene	25	4.3×10^{-1} (0.999)	1.25 [25] (0.996)	$Ru^{IV}(TPFPP)(O)$	2.9 [58]

[a] k_{cat}, conservative, hypothetical estimates calculated assuming that $Ru^{VI}(TPFPP)(O)_2$ is the only active oxidant and its concentration is equal to the initial concentration during the catalytic reactions. The values in brackets are catalytic rate constants assuming 5% active species. [b] Determined by ^1H NMR or UV−vis spectroscopy.

rate (eq 2). The data show that the turnover rate is much too fast for this hypothetical situation to be true, and accordingly, $Ru^{VI}(TPFPP)(O)_2$ cannot be the active catalytic oxidant.

$$\text{Rate} = -\text{d[substrate]}/\text{d}t = k_{cat}[\text{substrate}][Ru^{VI}(TPFPP)(O)_2]$$

$$[Ru^{VI}(TPFPP)(O)_2] = [Ru^{VI}(TPFPP)(O)_2]_0 \qquad (2)$$

Comparison of the catalytic and stoichiometric rate constants for the series of substrates in Table 3 shows that the catalytic rate constants (k_{cat}) are all significantly *larger* than the corresponding rate constants for the stoichiometric reactions of $Ru^{VI}(TPFPP)(O)_2$. For example, the rate constant for the stoichiometric reaction between $Ru^{VI}(TPFPP)(O)_2$ and *cis*-decalin (k_{st}) was determined to be 2.3×10^{-3} M^{-1} s^{-1} (25 °C). ^1H NMR monitoring of the catalytic oxidation of *cis*-decalin revealed that $Ru^{VI}(TPFPP)(O)_2$ remained the major porphyrin species during the reaction. If one assumes that *trans*-dioxoRu(VI) is the only active species under the catalytic conditions, the kinetics of the catalytic hydroxylation of *cis*-decalin in the presence of 2,6-dichloropyridine *N*-oxide would give $k_{cat} = 1.9 \times 10^{-2}$ M^{-1} s^{-1} (25 °C), which is more than 8 times greater than k_{st}. Such a substantial difference in the rate of oxidation under the stoichiometric and catalytic conditions indicates that the rate of catalytic oxidation cannot be explained if the *trans*-dioxoRu(VI) porphyrin is the only active oxidant. Some other ruthenium species with significantly higher activity than that of $Ru^{VI}(TPFPP)(O)_2$ must be involved in ruthenium porphyrin catalysis with 2,6-dichloropyridine *N*-oxide as an oxygen donor.

It is important to emphasize that the catalytic rate constants (k_{cat}) determined above represent very conservative estimates of the true catalytic rate constants, because the fraction of ruthenium porphyrin directly involved in the "fast" catalytic cycle is certainly much smaller than the initial concentration of the ruthenium porphyrin that was used for the calculation of k_{cat}. Indeed, the very modest changes in the visible spectra of the catalysts under turnover conditions indicate that the active species could never amount to more than ca. 5% of the catalyst inventory.

Redox Activation of $Ru^{II}(TPFPP)(CO)$ and $Ru^{IV}(TPFPP)Cl_2$. Important clues regarding the mechanism of this fast oxidative catalysis were obtained from observing the activation of the catalyst by redox processes. As mentioned above, oxygen eliminated the induction period observed when methylene chloride was the reaction solvent. Significantly, we have found that oxygen had no obvious effect on the rate of reaction with trifluorotoluene as the solvent. These observations and the slow rate of adamantane hydroxylation in the presence of cyclohexene (a stabilizer for methylene chloride)[43] are consistent with a component to the activation of $Ru^{II}(TPFPP)(CO)$ that involves *autoxidation of the solvent*.[44]

Scheme 3. Pathways Leading to Ru(III) Porphyrins from $Ru^{II}(TPFPP)(CO)$ and $Ru^{IV}(TPFPP)Cl_2$ (OD = 2,6-Dichloropyridine-*N*-oxide)

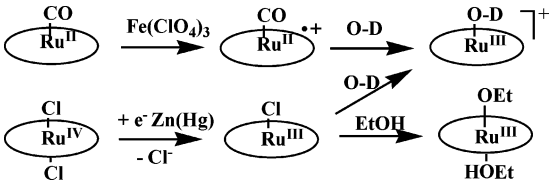

The activation of $Ru^{II}(TPFPP)(CO)$ that is observed by one-electron oxidation supports this hypothesis. We have previously reported the oxidation of $Ru^{II}(TPFPP)(CO)$ with $Fe(ClO_4)_3$ to the corresponding porphyrin cation radical, $Ru^{II}(TPFPP^{+\bullet})(CO)$ ($\lambda_{max} = 635$ nm).[27] The addition of lutidine-*N*-oxide to $Ru^{II}(TPFPP^{+\bullet})(CO)$ gave EPR signals characteristic of Ru(III). The hydroxylation of adamantane in methylene chloride with $Ru^{II}(TPFPP)(CO)$ pretreated with $Fe(ClO_4)_3$ proceeded without an induction period (Scheme 3).

We found that $Ru^{IV}(TPFPP)Cl_2$ is a faster catalyst than $Ru^{II}(TPFPP)(CO)$ or $Ru^{VI}(TPFPP)(O)_2$ and that it can be further activated by methylene chloride/air. The hydroxylation of adamantane in methylene chloride catalyzed by Ru^{IV}-

(43) Commercial methylene chloride contains 40−100 ppm (~1 mM) of cyclohexene or amylene as stabilizing agents against autoxidation. We found that the presence of even trace amounts of cyclohexene in the solvent caused prolonged induction periods and inhibited the catalytic hydroxylations of alkanes. Maximum turnover rates for cyclohexene epoxidation were 3 times slower than that of adamantane under comparable conditions even though cyclohexene was found to be 100 times intrinsically more reactive than adamantane in an intermolecular competition. The situation in benzene would appear to require some autoxidation of the substrate for catalyst activation.

(44) Yin, C.-X.; Sasaki, Y.; Finke, R. G. *Inorg. Chem.* **2005**, *44*, 8521−8530.

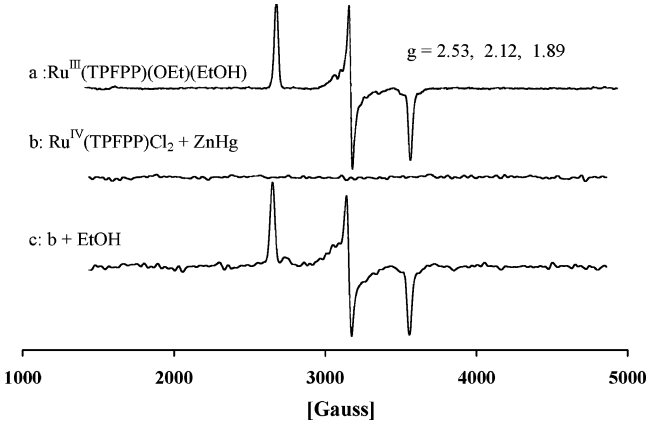

Figure 5. X-band EPR characterization of Ru^{III}(TPFPP) generated by the reduction of Ru^{IV}(TPFPP)$(Cl)_2$ with Zn(Hg). $T = 77$ K. (a) Ru^{III}(TPFPP)(OEt)(EtOH) in ethanol glass. (b) Ru^{IV}(TPFPP)Cl_2 reacted with Zn(Hg) in CD_2Cl_2 and quenched with liquid N_2. (c) After the addition of 10 μL of ethanol into 0.5 mL of solution b and quenched with liquid N_2.

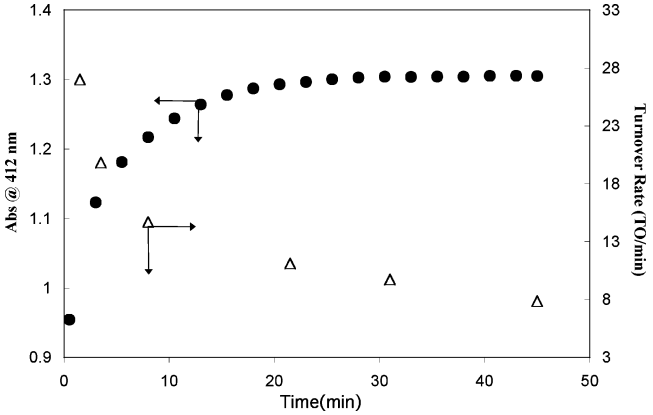

Figure 6. Kinetics of Ru^{III}(TPFPP)(OEt)(EtOH)-mediated adamantane hydroxylation with 2,6-dichloropyridine *N*-oxide followed with GC and UV−vis. Adamantane, 0.02 M; Ru^{III}(TPFPP)(OEt)(EtOH), 7.5 μM; 2,6-dichloropyridine *N*-oxide, 0.01 M; CH_2Cl_2; 25 °C.

$(TPFPP)Cl_2$ proceeded at a maximum rate of 6.3 TO/min under argon and 11.5 TO/min under air at 25 °C (Table 2, entries 2 and 3). Both rates were faster than the maximum turnover rates for $Ru^{VI}(TPFPP)(O)_2$- and Ru^{II}(TPFPP)(CO)-catalyzed reactions under identical conditions (0.39 and 0.43 TO/min, respectively, see Table 2, entries 6 and 7). On the other hand, the $Ru^{IV}(TPFPP)Cl_2$-mediated oxidation proceeded much slower in α,α,α-trifluorotoluene with a rate of 5.1 TO/min under air and 4.6 TO/min under argon (Table 2, entries 4 and 5). These observations strongly suggest that methylene chloride is involved in the activation of the catalyst.

The addition of a zinc amalgam to the reaction mixture of a $Ru^{IV}(TPFPP)Cl_2$-catalyzed oxidation of adamantane led to a sustained initial reaction rate *5 times faster* than that observed with $Ru^{IV}(TPFPP)Cl_2$ alone (31.4 TO/min vs 6.3 TO/min; see entries 1 and 2 in Table 2). Other additives such as $AgBF_4$, $AgPF_6$, trifluoroacetic acid, ferrocene, methanol, Bu_4NCl, and Me_4NOH slowed the catalytic oxidations. This activation by a zinc amalgam is consistent with a one-electron reduction of the Ru(IV) porphyrin to give a Ru(III) species in situ.

Indeed, proof of the formation of Ru(III) from $Ru^{IV}(TPFPP)Cl_2$ by zinc amalgam reduction was obtained by EPR spectroscopy. Thus, the reaction of $Ru^{IV}(TPFPP)Cl_2$ with a zinc amalgam in CH_2Cl_2 at 25 °C for 20 min caused a shift in the visible spectrum in the Q-band region from 506 to 520 nm. This solution was EPR-silent (Figure 5, trace b), and the NMR absorbance for the pyrrole protons of $Ru^{IV}(TPFPP)Cl_2$ (δ −53) was no longer apparent. The addition of ethanol at 25 °C caused the immediate appearance of a UV spectrum characteristic of an ethoxyRu(III) complex.[38,45,46] An NMR resonance at δ −15 and strong, sharp EPR signals (g = 2.53, 2.12, and 1.89) (Figure 5, trace c) observed in this solution at 77 K provide conclusive evidence for the presence of a Ru(III) complex in this sample (Scheme 3). No EPR signals were observed when ethanol was added to $Ru^{IV}(TPFPP)Cl_2$ even after 3 h at 25 °C.

Interestingly, when authentic Ru^{III}(TPFPP)(OEt) was used as the catalyst, the maximum turnover rate of adamantane oxidation at 25 °C at 7.5 μM catalyst was found to proceed at 28.8 TO/min, several times faster than the reactions mediated by Ru^{II}(TPFPP)(CO) or $Ru^{VI}(TPFPP)(O)_2$. Soon after the reaction started, the Ru^{III} species was gradually converted to a dioxo Ru^{VI} species, and the turnover rates in this process decreased concomitantly (Figure 6). This decrease in rate, accompanied by the conversion of Ru^{III} to Ru^{VI}, speaks against $Ru^{VI}(TPFPP)(O)_2$ as the active oxidant.

The kinetic and spectroscopic results described above have ruled out both $Ru^{VI}(TPFPP)(O)_2$ and Ru^{II}(TPFPP)(CO) as the active species in the "fast catalysis" regime for these hydroxylations and epoxidation reactions. Activation of the catalyst either by the oxidation of Ru^{II}(TPFPP)(CO) with $Fe(ClO_4)_3$ or the reduction of $Ru^{IV}(TPFPP)Cl_2$ to Ru(III) with a zinc amalgam or air/methylene chloride strongly supports the formation of Ru(III) in the catalyst activation process.

Proposed Catalytic Cycle. A mechanism that is consistent with the data described above is presented in Scheme 4. To explain the oxidation of hydrocarbons with the highest turnover rates and efficiencies, we propose Ru(III) and oxoRu(V) porphyrin species as the key intermediates. In this scenario, one-electron redox processes involving the inventory of Ru(II), Ru(IV), or Ru(VI) porphyrin species observed during catalysis would produce a low steady-state concentration of Ru(III) that is oxidized to oxoRu(V) by dichloropyridine-*N*-oxide. This interpretation differs from that of Hirobe et al., who have suggested that the dichloroRu(IV) porphyrin is a precursor of chloro,oxoRu(VI) cationic species,[24] and that of Gross et al.,[47] who have suggested an adduct of the oxoRu(IV) with the pyridine-*N*-oxide.

The "fast" catalytic pathway can be conveniently described using the terminology of chain-reaction kinetics, which includes initiation, propagation, and termination steps. The presence of an induction period in the kinetic profiles of the product evolution of the catalytic oxidations with Ru-

(45) Collman, J. P.; Rose, E.; Venburg, G. D. *J. Chem. Soc.* **1994**, 11−12.
(46) James, B. R.; Dolphin, D.; Leung, T. W.; Einstein, F. W. B.; Willis, A. C. *Can. J. Chem.* **1984**, *62*, 1238−1245.
(47) Gross, Z.; Ini, S. *Inorg. Chem.* **1999**, *38*, 1446−1449.

Scheme 4. Mechanisms of Hydrocarbon Oxygenation by Ru(TPFPP)

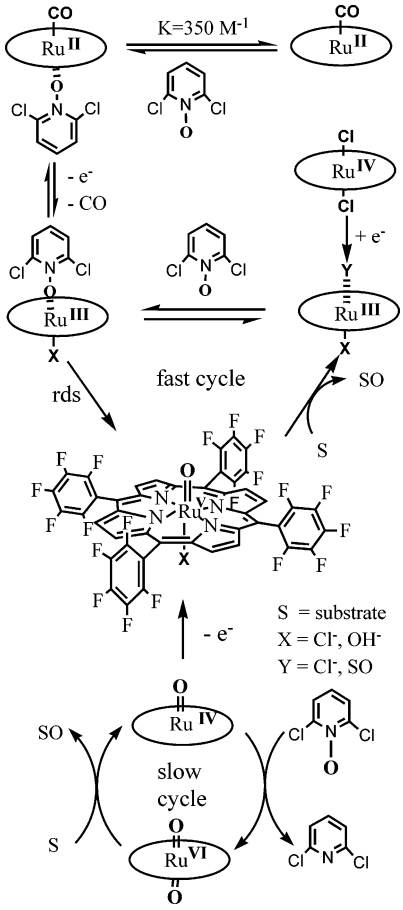

(TPFPP)/2,6-dichloropyridine *N*-oxide is an indication of an initiation process. During the initiation phase, a buildup of the metastable and highly catalytically active Ru(III) porphyrin would occur from the resting pool of ruthenium porphyrin catalyst represented by $Ru^{VI}(TPFPP)(O)_2$, Ru^{IV}-(TPFPP)(O), $Ru^{IV}(TPFPP)Cl_2$, or $Ru^{II}(TPFPP)(CO)$. During the propagation phase, the hydrocarbon substrates would be efficiently oxidized within the "fast" catalytic cycle with the oxoRu(V) porphyrin species formed via oxygen transfer from the pyridine *N*-oxide ligated to the Ru(III) precursor. Such a steady-state regime is uniquely consistent with the apparently zero-order kinetics observed for the product evolution.

It was observed that the maximum turnover rates obtained for the oxygenation of adamantane (at 72 TO/min) and *trans*-β-methylstyrene (at 45 TO/min)[48] differed only by a factor of 1.5. However, in the competitive oxidation of these two substrates, *trans*-β-methylstyrene was 50 times more reactive than adamantane under the same conditions. This observation provides support for the argument that the hydrocarbon substrates are discriminated *after* the rate-limiting step, and it is the formation of the oxoruthenium(V) intermediate from a Ru(III)-O-pyridine precursor that is rate-limiting (Figure 7). Furthermore, a *common active intermediate* is indicated for both the alkane hydroxylation and epoxidation of olefins in the Ru(TPFPP)/2,6-dichloropyridine *N*-oxide catalytic system.

(48) Wang, C.; Groves, J. T. Unpublished results.

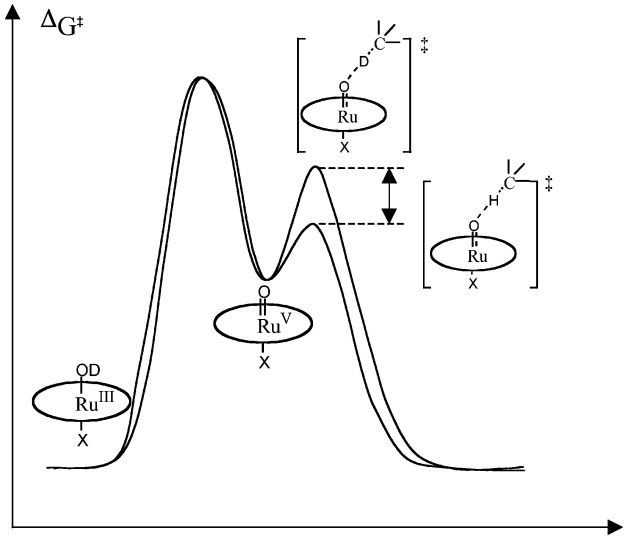

Figure 7. Energy diagram consistent with a large deuterium isotope effect in the competitive hydroxylation of adamantane and adamantane-d_{16} and a similar turnover observed in separate hydroxylations of adamantane and adamantane-d_{16}. The axial ligand, OX, is the pyridine *N*-oxide.

In the termination step, the Ru(III) and oxoRu(V) porphyrin species either return to the resting pool of the catalyst or the porphyrin macrocycles get oxidatively destroyed. The maximum number of catalytic turnovers obtained was found to increase only slightly as the concentration of the catalyst was decreased, suggesting an intramolecular self-oxidation as opposed to intermolecular deactivation pathways such as bimolecular oxidative cleavage of the porphyrin macrocycle and formation of inactive μ-oxo ruthenium porphyrin dimers.[38,49] The kinetics of oxidation of relatively unreactive substrates, such as cyclohexane, were affected by the oxidative bleaching of the porphyrin to a greater extent because the reactive oxoRu(V) intermediate would be longer-lived and more susceptible to decomposition. This need for "substrate rescue" of the catalyst is why such high concentrations of cyclohexane (2 M) were required to maintain the fast catalysis. Indeed, in the absence of a substrate, the ruthenium porphyrin was bleached completely in only a few minutes.

The even-number oxidation states of ruthenium, oxoRu-(IV) and *trans*-dioxoRu(VI) porphyrins, are known to be involved in a "slow" oxidation pathway. We have previously described a catalytic cycle, mediated by Ru(II), oxoRu(IV), and *trans*-dioxoRu(VI) porphyrins, for the aerobic epoxidation of olefins.[18,50,51] The oxidation of the substrate with Ru^{VI}-$(TPFPP)(O)_2$ would result in the formation of $Ru^{IV}(TPFPP)$-(O). $Ru^{IV}(TPFPP)(O)$ can either be directly reoxidized to a *trans*-dioxoRu(VI)porphyrin by 2,6-dichloropyridine *N*-oxide or undergo bimolecular disproportionation to give *trans*-dioxoRu(VI) and Ru(II) porphyrin complexes with subse-

(49) James, B. R.; Shilov, A. E. *Fundamental Research in Homogeneous Catalysis*; Gordon & Breach: New York, 1986; p 309.
(50) Groves, J. T.; Shalyaev, K.; Lee, J.; Kadish, K. M.; Smith, K. M.; Guilard, R. *The Porphyrin Handbook*; Academic Press: San Diego, 2000; Vol. 4, pp 17−40.
(51) Quici, S.; Banfi, S.; Pozzi, G. *Gazz. Chim. Ital.* **1993**, *123*, 597−612.

Table 4. Deuterium Isotope Effects[a]

catalyst	oxidant	substrate	solvent	*T*, °C	DIE
$Ru^{VI}(TPFPP)(O)_2$	$pyCl_2$ *N*-oxide	cyclohexane	CH_2Cl_2	25	4.5
$[Ru^{V}L_4(O)]^{2+}$		cyclohexane	CH_3CN	17	5.3 ± 0.6[36]
$Ru^{VI}(TPFPP)(O)_2$	$pyCl_2$ *N*-oxide	adamantane	CH_2Cl_2	25	5.2
$Ru^{VI}(TPFPP)(O)_2$	$pyCl_2$ *N*-oxide	adamantane	CH_2Cl_2	65	4.2
$Ru^{VI}(TPFPP)(O)_2$	$pyCl_2$ *N*-oxide	*cis*-decalin	CH_2Cl_2	40	5.5
$Ru^{VI}(TPFPP)(O)_2$	$pyCl_2$ *N*-oxide	*cis*-decalin	CH_2Cl_2	25	6.4
$Ru^{VI}(TPFPP)(O)_2$		*cis*-decalin	CH_2Cl_2	25	6.5
$Ru^{VI}(TPFPP)(O)_2$	$pyCl_2$ *N*-oxide	cyclohexanol	CH_2Cl_2	40	5.4
$[Ru^{V}L_4(O)]^{2+}$		propan-2-ol	H_2O	25	5.3 ± 0.5[36]
$[Ru^{IV}(trpy)(bpy)O]^{2+}$		propan-2-ol	H_2O	25	18 ± 3[37]
$[MnO_4]^-$		toluene	H_2O	20	9.7[38]
$[MnO_4]^-$		toluene	toluene	45	6[39]

[a] HL_4 = [2-hydroxy-2-(2-pyridyl)ethyl]bis[2-(2-pyridyl)ethyl] amine].

quent reoxidation of the Ru(II) porphyrin to $Ru^{IV}(TPFPP)(O)$. The contribution of this "slow" catalytic cycle toward the oxygenation of alkanes is small, given the slow stoichiometric rate constants reported here, but it cannot be entirely excluded, especially for the substrates such as olefins, which have relatively high intrinsic activity toward $Ru^{VI}(TPFPP)(O)_2$.

Nature of the Active Oxidant Species. Several mechanistic probes have been employed to elucidate the nature of the proposed oxoRu(V) intermediate in these catalytic oxygenations.

Deuterium Isotope Effect Studies. The competitive oxidation of a 1:1 mixture of adamantane and adamantane-d_{16} with 2,6-dichloropyridine-*N*-oxide catalyzed by $Ru^{VI}(TPFPP)(O)_2$ showed a kinetic isotope effect, $k_H/k_D = 4.8$ at 40 °C. However, the deuterated and undeuterated substrates displayed virtually no difference in the *turnover rates* of hydroxylation in separate reactions ($k_H/k_D = 1.2$). We have previously reported similar results obtained with a $Ru^{II}(TPFPP)(CO)$ catalyst.[27] Likewise, the catalytic oxidations of *cis*-decalin and *cis*-decalin-d_{18} with $Ru^{VI}(TPFPP)(O)_2$ used as catalyst proceeded with the same turnover rate, although $k_H/k_D = 5.5$ at 40 °C was measured in a competitive oxidation. Similar to the adamantane/*trans*-β-methylstyrene case discussed above, these deuterium isotope effect data are consistent with a process in which the active oxidant species, an oxoRu(V) porphyrin, is formed *in the rate-determining step* and differentiation of substrates occurs *after the rate-determining step* on the reaction coordinate (Figure 7). The deuterium isotope effect for the competitive, stoichiometric oxidation of *cis*-decalin and *cis*-decalin-d_{18} with $Ru^{VI}(TPFPP)(O)_2$ was 6.5 at 25 °C. The catalytic hydroxylation of *cis*-decalins with 2,6-dichloropyridine *N*-oxide mediated by a *trans*-dioxoRu(VI) complex gave a very similar value, $k_H/k_D = 6.4$.

Larger deuterium isotope effects than these values have been reported for the competitive oxidation of cyclohexanes with electron-deficient iron porphyrins, $Fe^{III}(TDCPP)/PhIO$ ($k_H/k_D = 9 \pm 3$) and $Fe^{III}(TMPBr_8)/PhIO$ ($k_H/k_D = 7.7 \pm 0.6$).[34] Smaller deuterium isotope effects have been measured for the manganese porphyrin catalyzed hydroxylation of cyclohexane with $Mn^{III}(TDCPP)/PhIO$ ($k_H/k_D = 2.6 \pm 0.4$; Table 4).[34]

Reliably characterized ruthenium(V) complexes and, especially, oxoruthenium(V) species are rare.[5,52,53] One of the few known examples of an oxoRu(V) complex is $[Ru^{V}L(O)]^{2+}$ {HL = [2-hydroxy-2-(2-pyridyl)ethyl]bis[2-(2-pyridyl)ethyl] amine]}, reported by Che et al.[54−56] Several characteristics of this complex are strikingly reminiscent of the reactivity features of the oxoRu(V) active species that we propose.[57−59] $[Ru^{V}L(O)]^{2+}$ is one of the fastest and most reactive oxoruthenium species toward stoichiometric C−H bond oxidation, capable of oxidizing cyclohexane under mild conditions similar to the behavior seen for the proposed oxoRu(V) porphyrin. Further, the kinetic isotope effect ($k_H/k_D = 5.3$) for cyclohexane oxidation with $[Ru^{V}L(O)]^{2+}$ is similar to the values we find for adamantane hydroxylation ($k_H/k_D = 5.2$) and cyclohexane hydroxylation ($k_H/k_D = 4.5$) with a Ru(TPFPP)/2,6-dichloropyridine *N*-oxide system.

Electronic Effects. The electronic features of the catalytic oxygenations have been probed through studies of the relative reactivity of substituted toluenes. A typical Hammett treatment of data for the hydroxylation of para-substituted toluenes in the Ru(TPFPP)/2,6-dichloropyridine *N*-oxide system produced an extraordinarily negative $\rho^+ = -2.0$ at 40 °C (Figure 8). This value is much greater than that for the relative rates of the competitive oxidation of toluenes by an oxoFe(IV) porphyrin radical cation, $Fe^{IV}(TPP^{+\bullet})(O)$, the active oxidant in the $Fe^{III}(TPP)Cl/PhIO$ system ($\rho^+ = -0.83$).[60] For typical radical reactions such as hydrogen-atom abstraction from $XC_6H_4CH_3$ by *t*-butoxy radicals and bromine atoms, ρ^+ values of −0.4 and −1.4, respectively, have been reported.[36] The large negative value of ρ^+ for the ruthenium-catalyzed process indicates an unusually high charge separation and electrophilic nature of the oxygen transfer step in the transition state of the "fast" ruthenium

(52) Dengel, A. C.; Griffith, W. P. *Inorg. Chem.* **1991**, *30*, 869−871.
(53) Fackler, N. L. P.; Zhang, S. S.; O'Halloran, T. V. *J. Am. Chem. Soc.* **1996**, *118*, 481−482.
(54) Che, C. M.; Wong, K. Y.; Mak, T. C. W. *J. Chem. Soc.* **1985**, 988−990.
(55) Che, C. M.; Yam, V. W. W.; Mak, T. C. W. *J. Am. Chem. Soc.* **1990**, *112*, 2284−2291.
(56) Che, C. M.; Ho, C.; Lau, T. C. *J. Chem. Soc., Dalton Trans.* **1991**, 1259−1263.
(57) Thompson, M. S.; Meyer, T. J. *J. Am. Chem. Soc.* **1982**, *104*, 5070−5076.
(58) Gardner, K. A.; Mayer, J. M. *Science* **1995**, *269*, 1849−1851.
(59) Gardner, K. A.; Kuehnert, L. L.; Mayer, J. M. *Inorg. Chem.* **1997**, *36*, 2069−2078.
(60) Inchley, P.; Lindsay-Smith, J. R.; Lower, R. J. *New J. Chem.* **1989**, *13*, 669−676.

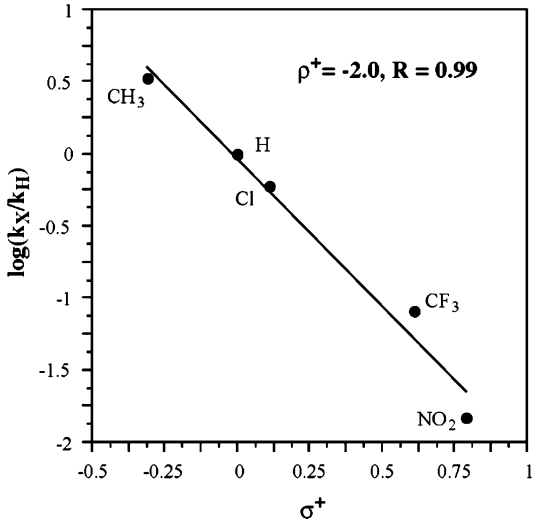

Figure 8. Hammett correlation of log k_{rel} for Ru^{II}(TPFPP)(CO)-catalyzed oxidations of para-substituted toluenes by 2,6-dichloropyridine *N*-oxide. Pairs of competing substrates (0.02 M) were oxidized with 2,6-dichloropyridine *N*-oxide (0.02 M) in the presence of Ru^{II}(TPFPP)(CO) (50 μM) in CH_2Cl_2 at 40 °C. The consumption of the substrates was followed by GC using 1,2-dichlorobenzene (0.01 M) as an internal standard.

catalysis compared to the characteristics of other metalloporphyrin systems.

Oxidation in the Presence of CCl_3Br. The catalytic oxidation of cyclohexane in 20% CCl_3Br/80% CH_2Cl_2 gave cyclohexanol (18% based on the oxidant) and cyclohexanone (55%), with only a small amount of bromocyclohexane (0.9%). The formation of brominated products in the presence of CCl_3Br has been used as evidence for the involvement of alkyl radical intermediates, because it is known that bromotrichloromethane reacts rapidly and efficiently with alkyl radicals to form alkyl bromides.[61] For example, the oxidation of cycloheptane by iodosylbenzene and Fe^{III}(TPP)Cl in the presence of bromotrichloromethane produced 24% cycloheptanol and an 18% yield of cycloheptyl bromide.[33] Lindsay-Smith et al.[60] reported that for Fe^{III}(TPP)Cl/PhIO oxidation approximately half of the starting material was diverted to bromocyclohexane, and in the case of the Mn^{III}(TPP)Cl-catalyzed reaction, bromotrichloromethane trapped 90% of the reacting cyclohexane.

The results presented here indicate that long-lived alkyl radicals are not formed during hydrocarbon oxygenations with the Ru(TPFPP)/2,6-dichloropyridine *N*-oxide catalytic system. First, the amount of cyclohexyl bromide formed in the oxidation of cyclohexane in the presence of bromotrichloromethane is negligible. Second, the hydroxylation of *cis*-decalin gave the retention products, *cis*-9-decalol and *cis*-decalin-9,10-diol, exclusively. The *cis*-9-decalyl radical is known to isomerize to the trans conformation with a rate in excess of 10^8 s^{-1}.[61b] Finally, the oxidation of cyclobutanol did not produce the ring-opening products characteristic of a one-electron oxidation step. Mayer et al. have reported recently that C−H bond oxidations by oxoRu(IV) complexes are initiated by hydrogen abstraction.[62,63] In these cases, the carbon radicals are long-lived enough to dimerize and disproportionate via intermolecular reactions. By contrast, the oxoRu(V) species proposed here is behaving very differently, with no evidence of radical species that live long enough to be trapped. Thus, if these reactions do proceed via the prototypical oxygen rebound pathway, the intermediate geminate radical pair [Ru(IV)−OH •R] must collapse in the solvent cage with very high efficiency.

^{18}O exchange. ^{18}O incorporation in the oxidation products for hydrocarbon oxygenations mediated by metalloporphyrins has been widely used to implicate metal-oxo species as the oxygen transfer agents.[64−68] The hydroxylation of adamantane catalyzed by Ru^{VI}(TPFPP)$(O)_2$ in the presence of $H_2{}^{18}O$ (92%) led to an 18% incorporation of the ^{18}O label from the moist CH_2Cl_2 into the product, 1-adamantanol. By contrast, 3.4% ^{18}O incorporation into 1-adamantanol was observed with Ru^{II}(TPFPP)(CO) as the catalyst. This result supports the hypothesis that the pyridine *N*-oxide reacts to form an oxoruthenium porphyrin species, such as oxoRu(V), that is capable of exchange with water. The relatively low degree of ^{18}O exchange into the product, especially when Ru^{II}(TPFPP)(CO) was used as the catalyst, is consistent with a short lifetime of the highly active oxidant species.[69] As discussed above, the oxidations mediated by Ru^{II}(TPFPP)(CO) and Ru^{VI}(TPFPP)$(O)_2$ have similar turnover rates (see Table 2) but with Ru^{VI}(TPFPP)$(O)_2$ having much higher ^{18}O incorporation. The majority of the ^{18}O incorporation in the hydroxylation of adamantane mediated by Ru^{VI}(TPFPP)$(O)_2$ should be due to the "slow" catalytic cycle [dioxoRu(VI) to oxoRu(IV)]. It is also known that the oxoRu(IV) complexes undergo rapid oxygen exchange with water.[70]

Reactivity and Selectivity. The high 3°/2° selectivity observed in the hydroxylation of adamantane is in contrast with the far less selective hydrocarbon oxidations catalyzed by iron and manganese porphyrins.[33,34] The possible explanation for such a difference in selectivity can be derived from a Hammond postulate reasoning. The oxoRu(V) species is expected to be lower in free energy than the corresponding oxoMn(V)[71] and oxoFe(IV)(porphyrins$^{+\bullet}$).[72,73] Accordingly, the reactive oxoRu(V) intermediate would interact with a

(61) (a) Huyser, E. S.; Burham, R. L.; Schimke, H. *J. Org. Chem.* **1963**, *28*, 2141. (b) Hummel, A.; Deleng, H. C.; Luthjens, L. H. *Radiat. Phys. Chem.* **1995**, *45*, 745−748 and references therein.

(62) Bryant, J. R.; Mayer, J. M. *J. Am. Chem. Soc.* **2003**, *125*, 10351−10361.
(63) Bryant, J. R.; Matsuo, T.; Mayer, J. M. *Inorg. Chem.* **2004**, *43*, 1587−1592.
(64) Groves, J. T.; Stern, M. K. *J. Am. Chem. Soc.* **1988**, *110*, 8628−8638.
(65) Groves, J. T.; Stern, M. K. *J. Am. Chem. Soc.* **1987**, *109*, 3812−3814.
(66) Groves, J. T.; Lee, J. B.; Marla, S. S. *J. Am. Chem. Soc.* **1997**, *119*, 6269−6273.
(67) Pitie, M.; Bernadou, J.; Meunier, B. *J. Am. Chem. Soc.* **1995**, *117*, 2935−2936.
(68) Bernadou, J.; Fabiano, A. S.; Robert, A.; Meunier, B. *J. Am. Chem. Soc.* **1994**, *116*, 9375−9376.
(69) Nam, W. W.; Valentine, J. S. *J. Am. Chem. Soc.* **1993**, *115*, 1772−1778.
(70) Ahn, K. H. Ph.D. Thesis, Princeton University, Princeton, New Jersey, 1988.
(71) Jin, N.; Bourassa, J. L.; Tizio, S. C.; Groves, J. T. *Angew. Chem., Int. Ed.* **2000**, *39*, 3849−3851.
(72) Holm, R. H. *Chem. Rev.* **1987**, *87*, 1401−1449.
(73) Holm, R. H.; Donahue, J. P. *Polyhedron* **1993**, *12*, 571−589.

hydrocarbon substrate leading to a comparatively late, product-like transition state while the more reactive oxomanganese and oxoiron species react via early transition states for C−H bond cleavage, resulting in a lower selectivity and stereospecificity.

We suggest that the apparent concertedness of the oxygenation reaction with this ruthenium system derives from both this late transition state and the strong preference of Ru to remain low-spin. Thus, a doublet d^3 ground state for oxoRu(V) could pass adiabatically to a doublet d^5 Ru(III) complex. The lack of a spin barrier during the transformation between $(d_{xy})^2(d_{xz})^1$ and $(d_{xy})^2(d_{xz})^2(d_{yz})^1$ electron configurations of ruthenium porphyrin in the oxoRu(V)−Ru(III) catalytic cycle might be a key to understanding the faster rates of hydrocarbon oxidation with this metastable redox couple compared to the rates of oxoRu(IV)/*trans*-dioxoRu(VI)-mediated reactions.[17,74−76] For example, we have shown that low-spin, d^2 oxoMn(V) porphyrin complexes do display large kinetic differences in reactivity, which we have attributed to the need to promote an electron from d_{xy} to produce *high-spin* Mn(IV) or Mn(III) states.[71,77]

Summary and Conclusions

We have shown that ruthenium complexes of 5,10,15,20-tetrakis(pentafluorophenyl)porphyrin are efficient catalysts for the oxygenation of a variety of substrates with 2,6-dichloropyridine *N*-oxide used as the oxidant. High rates and yields and large turnover numbers have been obtained with these catalysts under mild conditions in a nonacidic reaction medium.

The carbonylRu(II) and *trans*-dioxoRu(VI) porphyrin complexes have been excluded as the active species in this fast catalytic system, on the basis of comparative kinetic evidence. While $Ru^{VI}(TPFPP)(O)_2$ was found to be an effective oxidant, the rates of the stoichiometric oxidations were much too slow to explain the catalysis.

Free-radical processes of substrate oxygenation have been ruled out by the observed stereospecificity of the hydroxylation of decalin and the lack of brominated products with added $BrCCl_3$.

Catalyst activation was observed upon the oxidation of $Ru^{II}(TPFPP)(CO)$ with $Fe(ClO_4)_3$ to the corresponding porphyrin cation radical, $Ru^{II}(TPFPP^{+\bullet})(CO)$, or upon the reduction of $Ru^{IV}(TPFPP)Cl_2$ with a zinc amalgam. A Ru(III) porphyrin species was shown to be formed under these conditions.

$Ru^{III}(TPFPP)(OEt)$-mediated adamantane oxidation was found to proceed at a rapid initial rate, and then, gradually slowed as $Ru^{III}(TPFPP)$ was converted to $Ru^{VI}(TPFPP)(O)_2$. The observation confirms that $Ru^{VI}(TPFPP)(O)_2$ cannot be the active oxidant and that the Ru^{III} porphyrin is a precursor to the active oxidation species.

We propose a mechanism for the "fast" cycle mediated by highly active Ru(III) and oxoRu(V) species. A second, "slow" catalytic pathway involving *trans*-dioxoRu(VI) and oxoRu(IV) porphyrin complexes proceeds simultaneously.

Experimental Section

General. Analytical gas chromatography was performed on Hewlett-Packard 5890 gas chromatographs equipped with flame ionization detectors. SPB-20 and Stabilwax capillary columns were used. Mass spectra were taken on a Kratos MS50 RFA mass spectrometer with a FAB source. 3-Nitrobenzyl alcohol was used for the matrix. GC-MS data were obtained on a HP 5890A gas spectrometer equipped with an SPB-20 column and a HP 5970 series mass-selective detector. ^{1}H NMR spectra were taken on Varian INOVA 500 (500 MHz), JEOL GSX-270 (270 MHz), and Bruker WM 250 (250 MHz) spectrometers. Chemical shift values are reported relative to residual solvent resonances (δ 7.26, 5.32, and 1.11 for $CHCl_3$, $CHDCl_2$, and CHD_2CD_2OD, respectively). EPR spectra were recorded at 77 K on a Bruker ESP 300 X-band spectrometer using a low-temperature Dewar. UV−vis spectra were measured on a HP 8452A diode array spectrophotometer. IR spectra were taken on a Nicolet 5DXB FT-IR spectrometer.

Materials. Methylene chloride was purified to remove olefins by washing it with concentrated sulfuric acid, then aqueous sodium carbonate and water, followed by drying it over anhydrous $CaCl_2$ and distillation from CaH_2. Benzene (thiophene free grade) was distilled over sodium. Deuterated solvents, CD_2Cl_2, $CDCl_3$, and ethanol-d_6, were purchased from Aldrich or Cambridge Isotope Laboratories. $CDCl_3$ and CD_2Cl_2were purified by passage through a short column packed with basic alumina. *cis*-Decalin was purified by passage through basic alumina. $Ru_3(CO)_{12}$ purchased from Aldrich was purified by dissolution in hot toluene, filtration, and removal of the solvent. Free base 5,10,15,20-tetrakis(pentafluorophenyl)porphyrin, H_2TPFPP, was obtained from Mid-Century Chemicals and used without further purification. Zinc powder (20 mesh) was purchased from EM Science. A 200−400 mesh, 60 Å silica gel (Aldrich) was used for chromatographic separations. Basic alumina, Brockmann activity grade I (J. T. Baker), was treated with water (3 mL per 100 g of alumina) before use. All other reagents were purchased from Aldrich and used without further purification unless otherwise noted. Cyclopentyl acetate was prepared from cyclopentanol and acetic anhydride in the presence of $ZnCl_2$. Iodosylbenzene was prepared by the hydrolysis of iodobenzene diacetate.[78] $Ru^{II}(TMP)(CO)$[79] and $Ru^{II}(TPFPPBr_8)(CO)$[80,81] were synthesized according to published procedures.

Carbonyl(5,10,15,20-tetrakis(pentafluorophenyl)porphyrinato) Ruthenium(II) [$Ru^{II}(TPFPP)(CO)$].[82] H_2TPFPP (200 mg) and 100 mg of $Ru_3(CO)_{12}$ were refluxed in 30 mL of 1,2-dichlorobenzene under argon. After 3 h, another 100 mg portion of $Ru_3(CO)_{12}$ was added, and the reaction continued for 12 h. The solvent was removed under a vacuum, and the product was chromatographed with toluene on a silica gel column (Silica gel, Aldrich, 60−200 mesh, 5 × 20 cm). A bright orange band (R_f =

(74) Shaik, S.; Filatov, M.; Schroder, D.; Schwarz, H. *Chem.—Eur. J.* **1998**, *4*, 193−199.
(75) Hirao, H.; Kumar, D.; Thiel, W.; Shaik, S. *J. Am. Chem. Soc.* **2005**, *127*, 13007−13018.
(76) Sharma, P. K.; de Visser, S. P.; Ogliaro, F.; Shaik, S. *J. Am. Chem. Soc.* **2003**, *125*, 2291−2300.
(77) Jin, N.; Groves, J. T. *J. Am. Chem. Soc.* **1999**, *121*, 2923−2924.
(78) Lucas, H. J.; Kennedy, E. R. *Organic Structure*; Wiley: New York, 1955; Vol. 3.
(79) Groves, J. T.; Quinn, R. *Inorg. Chem.* **1984**, *23*, 3844−3846.
(80) Birnbaum, E. R.; Schaefer, W. P.; Labinger, J. A.; Bercaw, J. E.; Gray, H. B. *Inorg. Chem.* **1995**, *34*, 1751−1755.
(81) Mandon, D.; Ochsenbein, P.; Fischer, J.; Weiss, R.; Jayaraj, K.; Austin, R. N.; Gold, A.; White, P. S.; Brigaud, O.; Battioni, P.; Mansuy, D. *Inorg. Chem.* **1992**, *31*, 2044−2049.
(82) Murahashi, S. I.; Naota, T.; Komiya, N. *Tetrahedron Lett.* **1995**, *36*, 8059−8062.

0.39) was collected. Removal of the solvent yielded 165 mg (73%) of the product. ^{1}H NMR (CD_2Cl_2, 270 MHz): H_β δ 8.76. UV−vis (CH_2Cl_2): λ_{max} (log ϵ) 402 (5.45), 524 (4.29), 554 (4.00) nm.

***trans*-Dioxo(5,10,15,20-tetrakis(pentafluorophenyl)porphyrinato) Ruthenium(VI) [Ru^{VI}(TPFPP)(O)$_2$].** The solution of 27 mg of *m*-CPBA (57−87%) in 1.5 mL of CH_2Cl_2 was added to 40 mg (36.3 μmol) of Ru^{II}(TPFPP)(CO) dissolved in 5 mL of CH_2Cl_2. The reaction mixture was stirred for 2.5 min at room temperature and then applied to a jacketed silica gel column (1 × 10 cm, Silica Gel) cooled with a dry ice/acetone mixture. A fast-moving brown band was collected; the solvent was removed on a rotary evaporator, and the brown solid was dried under a vacuum (30.6 mg, 76%). ^{1}H NMR (CD_2Cl_2, 270 MHz): H_β δ 9.26. UV−vis (CH_2Cl_2): λ_{max} (log ϵ) 412 (5.35), 506 (4.18) nm. IR (KBr) ν_{RuO}: 826 cm^{-1}.

Dichloro(5,10,15,20-tetrakis(pentafluorophenyl)porphyrinato) Ruthenium(IV) [Ru^{IV}(TPFPP)Cl$_2$]. Ru^{IV}(TPFPP)Cl_2 was prepared both by refluxing Ru^{II}(TPFPP)(CO) in carbon tetrachloride in air, in a procedure similar to that described by Gross and Barzilay[83] and by the reaction of Ru^{VI}(TPFPP)$(O)_2$ with HCl. Both methods produced substantial amounts of μ-oxo dimer byproducts, [Ru^{IV}(TPFPP)X]$_2$O, along with Ru^{IV}(TPFPP)Cl_2.[38,83] The dichloroRu(IV) porphyrin could be easily isolated by refluxing the crude reaction mixture in a Soxhlet apparatus with diethyl ether, because the μ-oxo dimers were soluble in ether and Ru^{IV}(TPFPP)Cl_2 was not. Ru^{IV}(TPFPP)Cl_2 was EPR-silent. The position of its paramagnetically shifted pyrrole H (δ −53) in the ^{1}H NMR spectrum was close to those for the related complexes, Ru^{IV}(TMP)Cl_2 (δ −55.0),[70] Ru^{IV}(TDMPP)Cl_2 (δ −55.4), and Ru^{IV}(TPP)Cl_2 (δ −57.7).[83]

Method 1. Ru^{II}(TPFPP)(CO) (60 mg, 54.5 μmol) was dissolved in 250 mL of carbon tetrachloride in a 500 mL round-bottom flask equipped with a reflux condenser. The solution was refluxed for 4 h exposed to air. The color of the reaction mixture changed from bright orange to green. The solvent was removed on a rotary evaporator, and the solid was dried under a vacuum. The crude product was placed in a Soxhlet apparatus and extracted with diethyl ether for 8 h. A brown solid insoluble in ether was dried under a vacuum (32.8 mg, 53%).

Method 2. Anhydrous HCl gas was bubbled through a solution of 30 mg of Ru^{VI}(TPFPP)$(O)_2$ in 50 mL of CH_2Cl_2 for 30 min. After 12 h, the solvent was removed, and the brown solid was dried under a vacuum. The product was purified as described in method 1 (12.5 mg, 40%). NMR (CD_2Cl_2, 270 MHz): H_β δ −53. UV−vis (CH_2Cl_2): λ_{max} (log ϵ) 406 (5.25), 506 (5.07) nm.

2,6-Dichloropyridine *N*-Oxide. To 15 mL of trifluoroacetic acid was added 2.0 g (13.5 mmol) of 2,6-dichloropyridine in a 100 mL round-bottom flask. A total of 3 mL of 30% hydrogen peroxide was added dropwise, and the reaction was run at 75−80 °C for 5 h. Then, 1.5 mL of hydrogen peroxide was added, and the reaction was carried out for another 5 h. After that, the reaction was diluted with 20 mL of chloroform and quenched with 20 mL of a 5% aqueous sodium metabisulfate solution. Solid K_2CO_3 was added to neutralize the trifluoroacetic acid. The organic phase was separated, washed with water until a neutral reaction of the aqueous phase was established, and dried over anhydrous sodium sulfate. The solvent was removed on a rotary evaporator, and the solid product was purified by chromatography on a basic alumina column (4 × 7 cm, basic alumina was partially deactivated with 3% water by weight, eluent CH_2Cl_2). The first fast-moving band was unreacted 2,6-dichloropyridine. The second slow-moving band was collected, and 1.72 g (78%) of the product was obtained. ^{1}H NMR (CD_2Cl_2, 270 MHz): δ 7.10 (t, J = 8.6, 1 H), 7.46 (d, J = 8.6, 2 H).

General Procedure for Catalytic Oxidations. Most hydrocarbon oxidations were carried out in threaded 3.7 mL vials with an open-top closure and a PTFE-faced silicone septum. The measurements of volumes were done with gastight Hamilton syringes. The conditions for a typical reaction were as follows: the substrate (200 μL of 0.2 M in CH_2Cl_2), 2,6-dichloropyridine *N*-oxide (200 μL of 0.2 M in CH_2Cl_2), and 1,2-dichlorobenzene (100 μL of 0.2 M in CH_2Cl_2) were added to 1.4 mL of methylene chloride in a vial. The reaction solution was purged with argon for 5 min with a needle pierced through the septum. The vial was wrapped in aluminum foil to protect it from exposure to light and preheated in a thermostat for 10 min to the desired temperature. The reaction was initiated by the injection of 100 μL of 1 mM ruthenium porphyrin stock solution in CH_2Cl_2 into the vial. The porphyrin catalyst stock solution was also purged with argon for 5 min before use. A gas chromatographic analysis was performed on aliquots withdrawn directly from the reaction vessel. The yields and turnover numbers were determined against 1,2-dichlorobenzene used as an internal standard.

Maximum turnover numbers obtained for the hydroxylation of cyclohexane with 2,6-dichloropyridine *N*-oxide with several ruthenium porphyrin catalysts (10 μM) were compared {total TON = ([cyclohexanol] + 2[cyclohexanone])/[Ru catalyst]$_0$. [Cyclohexane] = 2.0 M, [2,6-dichloropyridine *N*-oxide] = 0.05 M, CH_2Cl_2, 65 °C}. Under these conditions, the reaction catalyzed by Ru^{II}(TMP)(CO) and Ru^{II}(TPFPPBr$_8$)(CO) gave 300 TO, Ru^{II}(TPFPP)(CO) afforded 2500 TO, and Ru^{II}(TPFPPBr$_8$)(CO) gave 5800 TO. Ru^{II}(TPFPPBr$_8$)(CO) was recharged with additional 0.05 M 2,6-dichloropyridine *N*-oxide.

For the reactions carried out in the presence of a zinc amalgam, 100 mg of the zinc amalgam and a small stirrer were introduced into the reaction vial. The reaction solution was rapidly stirred.

Competitive Oxidation of Hydrocarbons. Competition between pairs of substrates in catalytic oxidations were performed to determine the relative reactivities of different substrates as such as well as to measure the intermolecular deuterium isotope effects and obtain data for the Hammett correlations. In a typical experiment, the following stock solutions prepared in methylene chloride were added to 1.2 mL of CH_2Cl_2 in a 3 mL vial: substrate *a* (200 μL of 0.2 M), substrate *b* (200 μL of 0.2 M), 2,6-dichloropyridine *N*-oxide (200 μL of 0.2 M), and 1,2-dichlorobenzene (100 μL of 0.2 M). This mixture was purged with argon for 5 min and, after that, analyzed by gas chromatography at least three times to determine the exact initial concentrations of the substrates relative to the 1,2-dichlorobenzene internal standard. After that, the vial was preheated in a thermostat for 10 min, and 100 μL of 1 mM ruthenium porphyrin catalyst was injected. The final composition of the reaction mixture was analyzed by gas chromatography. At least three GC analyses were performed for each sample.

The relative reactivities of substrates *a* and *b*, $k_{rel} = k_a/k_b$, were calculated as follows:

$$k_{rel} = \ln([\text{substrate } a]/[\text{substrate } a]_0)/\ln([\text{substrate } b]/[\text{substrate } b]_0)$$

where [substrate *a*]$_0$ and [substrate *b*]$_0$ are the initial concentrations of the two substrates.

The relative reactivity of cyclohexanol versus that of cyclohexane was obtained from the kinetics of appearance of the products in

(83) Gross, Z.; Barzilay, C. M. *J. Chem. Soc., Chem. Commun.* **1995**, 1287−1288.

Table 5

time, min	cyclohexanol, mM (TO)	cyclohexanone, mM (TO)	$k_{cyclohexanol}/k_{cyclohexane}$
5	1.92 (192)	0.12 (12)	127.4
10	3.46 (346)	0.38 (38)	128.6
20	6.12 (612)	1.12 (112)	119.9
30	7.63 (763)	1.79 (179)	122.7
40	8.91 (891)	2.33 (233)	117.3
85	10.53 (1053)	3.48 (348)	125.4
103	10.80 (1080)	3.76 (376)	128.8
223	11.98 (1198)	4.45 (445)	124.0
268	12.54 (1254)	4.61 (461)	117.4
354	12.33 (1233)	4.62 (462)	121.6

the catalytic hydroxylation of cyclohexane (2.0 M) with 2,6-dichloropyridine *N*-oxide (0.05 M) catalyzed by 10 μM Ru^{II}(TPFPP)(CO) in CH_2Cl_2 at 65 °C following the general procedure. The concentrations of the oxidation products, cyclohexanol and cyclohexanone, were determined by gas chromatography at time intervals during the course of the reaction. 1,2-Dichlorobenzene (0.01 M) was used as an internal standard. Assuming that the same active oxidant is involved in the oxidation of both cyclohexane and cyclohexanol, the rate expressions can be written as follows:

$$d[\text{cyclohexanol}]/dt \approx k_{\text{cyclohexane}}[\text{cyclohexane}]\, f(X) \qquad \text{(I)}$$

where $k_{cyclohexane}$ and $k_{cyclohexanol}$ are absolute rate constants of

$$d[\text{cyclohexanone}]/dt = k_{\text{cyclohexanol}}[\text{cyclohexanol}]\, f(X) \qquad \text{(II)}$$

oxidation of cyclohexane and cyclohexanol, respectively, and f(X) is a substrate-independent component of the rate. The division of eq I by eq II and rearrangement followed by integration will give a time-independent expression:

$$k_{\text{cyclohexanol}}/k_{\text{cyclohexane}} = (2[\text{cyclohexane}][\text{cyclohexanone}])/[\text{cyclohexanol}]^2 \qquad \text{(III)}$$

Because $[\text{cyclohexane}]_0 \gg$ [2,6-dichloropyridine *N*-oxide], we can assume that [cyclohexane] $\approx [\text{cyclohexane}]_0$. Using formula III to calculate the relative reactivity of cyclohexane and cyclohexanol, $k_{cyclohexanol}/k_{cyclohexane}$ was found to be 123 ± 5 during the whole course of the oxidation (ca. 350 min). Data for these assays are shown in Table 5.

Hydroxylation of Adamantane in the Presence of $H_2{}^{18}O$. A 500 μL reaction mixture containing 20 μM Ru^{VI}(TPFPP)$(O)_2$ or Ru^{II}(TPFPP)(CO), 40 μM 2,6-dichloropyridine *N*-oxide, 20 mM adamantane, and 10 μL $H_2{}^{18}O$ was stirred at 25 °C under argon. Product development was monitored periodically by GC. Separate GC-MS analyses were performed on two reaction mixtures taken after 30% conversion to 1-adamantanol. To determine the ^{18}O content of the water, a 100 μL aliquot of each reaction mixture was treated with 0.4 μL of triethylorthopropionate and the ^{18}O content of the resultant ethyl propionate as determined by GC-MS. The ^{18}O content of the oxidation product, 1-adamantanol, was determined from the ratio of *m*/*e*, 152 and 154 after correction for the ^{18}O content. The ^{18}O incorporation in the 1-adamantol obtained from the oxidation catalyzed by Ru^{VI}(TPFPP)$(O)_2$ was found to be 18%. If Ru^{II}(TPFPP)(CO) was used as the catalyst, the ^{18}O incorporation in 1-adamantanol was 3.42%.

Kinetic Measurements. Oxidations were carried out as described in the general procedure. Aliquots of 30 μL were periodically withdrawn from a reaction, placed in small vials, and immediately frozen in liquid nitrogen. Later, the aliquots were defrosted and analyzed by gas chromatography one at a time.

In experiments on simultaneous monitoring of the product evolution and the fate of the porphyrin catalyst, the reactions were run directly in a 1-cm-path-length UV−vis cell with a threaded neck closed with an open-top cap and a PTFE-faced silicone septum. The reaction temperature was adjusted with a temperature control unit connected to the cell compartment of a spectrophotometer. The transformations of the catalyst were followed by UV−vis spectroscopy in the 450−650 nm range using a <430 nm cutoff filter placed in the light beam of the spectrophotometer. Aliquots of 30 μL were periodically withdrawn directly from the UV−vis cell at time intervals, frozen in liquid nitrogen, and later analyzed by GC in order to follow the evolution of the products of oxidation.

Stoichiometric Reactions of Ru^{VI}(TPFPP)$(O)_2$. A 2.2 mM solution of Ru^{VI}(TPFPP)$(O)_2$ and a 40 mM solution of *cis*-decalin in CD_2Cl_2 were prepared in an inert-atmosphere glovebox. The reaction was initiated by injecting 90 μL of a 40 mM solution of *cis*-decalin into 0.80 mL of a 2.2 mM solution of Ru^{VI}(TPFPP)$(O)_2$ in an NMR tube with a threaded neck covered with a screw cap and a PTFE-faced silicone septum. The disappearance of the β-pyrrole resonance of Ru^{VI}(TPFPP)$(O)_2$ was monitored at 25 °C, and the rate constant of the reaction was obtained from a single-exponential fit of the data. Control experiments in the absence of a substrate showed that catalyst decomposition was negligible in these runs. A similar procedure was used to determine the rate constant for the stoichiometric oxidation of styrene.

The reactions of the other substrates were studied by UV−vis spectroscopy. A total of 2.85 mL of the substrate solution (21.1 mM for adamantane, 42.1 mM for benzyl alcohol, and 2 M for cyclohexanol) was placed in a UV−vis cell and purged with argon for at least 5 min. The cell was equilibrated for 10 min to the desired temperature in the cell compartment of the spectrophotometer. A <430 nm cutoff filter was placed in the light beam to decrease the exposure of the sample to light. A 1.0 mM solution of Ru^{VI}(TPFPP)$(O)_2$ was prepared under argon. After the injection of 150 mL of Ru^{VI}(TPFPP)$(O)_2$ into the cell, an increase in absorbance at 450 nm followed. The rise in absorbance at this wavelength was due to the appearance of oxoRu(IV) porphyrin in the case of cyclohexanol and benzyl alcohol and to the formation of a μ-oxoRu(IV) dimer during adamantane oxidation. The rate constants (k_{st}) were obtained from a single-exponential fit of the data.

Catalytic Oxidation of *cis*-Decalin Followed by NMR. To 0.7 mL of a 2.86 mM solution of Ru^{VI}(TPFPP)$(O)_2$ in an NMR tube were injected 2,6-dichloropyridine *N*-oxide and *cis*-decalin (0.20 mL of 0.2 M). The course of the reaction was followed at 25 °C by monitoring the disappearance of 2,6-dichloropyridine *N*-oxide peaks and the appearance of the resonances of 2,6-dichloropyridine. A turnover rate of 0.045 TO/min for *cis*-decalin oxidation was determined from a linear fit of the data obtained during the first 250 min of the oxidation.

Formation of μ-Oxoruthenium(IV) Porphyrin Dimer [Ru^{IV}(TPFPP)(X)]$_2$O upon Decomposition of Ru^{VI}(TPFPP)$(O)_2$. Freshly prepared Ru^{VI}(TPFPP)$(O)_2$ (1 mg) was dissolved in 1 mL of CD_2Cl_2 and left at room temperature for 72 h. The reaction mixture was analyzed by ^1H NMR. 1H NMR (270 MHz): H_β δ 8.62. UV−vis (CH_2Cl_2): λ_{max} (log ϵ) 384 (5.28), 398 (5.21), 532 (4.42), 552 (4.38) nm. FAB-MS (3-nitrobenzyl alcohol as the matrix): cluster centered at *m*/*z* 2164 for [Ru(TPFPP)]$_2$O (observed relative intensity, calculated relative intensity), 2159 (31, 27), 2160 (45, 32), 2161 (65, 56), 2162 (77, 72), 2163 (91, 89), 2164 (100, 100), 2165 (82, 80), 2166 (73, 74), 2167 (48, 45).

Reduction of Dichloro(5,10,15,20-tetrakis(pentafluorophenyl)-porphyrinato) Ruthenium(IV) [Ru^{IV}(TPFPP)Cl_2] with a Zinc Amalgam. To 1 mL of 0.5 mM Ru^{IV}(TPFPP)Cl_2 in CD_2Cl_2, 100

mg of a freshly prepared zinc amalgam was added. The reaction mixture was stirred at 25 °C for 20 min under argon. The ^{1}H NMR spectrum taken at this point showed no resonances in the upfield region ($\delta < 0$) of the spectrum. No signals were apparent in the X-band EPR spectrum of this solution at 77 K. A 10 μL aliquot of ethanol-d_6 was added at 25 °C, and the NMR spectrum, taken after 15 min, displayed a typically broadened resonance at δ −15 characteristic of Ru^{III}(TPFPP)(OEt)(HOEt). The EPR spectrum of this solution at 77 K displayed a sharp, three-line signal at $g =$ 2.53, 2.12, and 1.89 as expected for a low-spin d^5 system. In a control experiment, the treatment of Ru^{IV}(TPFPP)Cl_2 with ethanol-d_6 under identical conditions but without a zinc amalgam treatment showed only the δ −53 resonance of the starting Ru(IV) porphyrin. The EPR spectrum was silent both 20 min and 3 h after the ethanol treatment.

Adamantane Oxidation Catalyzed by Ru^{III}(TPFPP)(OEt)(EtOH) Followed by GC and UV−vis Spectroscopy. The oxidation experiment was carried out in quartz UV cells with open-top, screw-cap, and Teflon-coated rubber septa. The UV−vis spectra were recorded in cycle mode with the temperature maintained at 25 °C. Reaction time was measured from the addition of the substrate and the oxidant. At regular intervals, an aliquot (30 μL) was withdrawn for GC analysis. The reaction mixture was prepared with Ru^{III}(TPFPP)(OEt)(EtOH) as a catalyst (7.5 μM), a substrate (0.02 M), an oxidant (0.01 M), 1,2-dichlorobenzene as a GC internal standard (0.01 M), and methylene chloride (2 mL) as the solvent.

Acknowledgment. The National Science Foundation (CHE-316301) for support of this research, the Monsanto Company for fellowship support to K.V.S., and Bayer, AG for partial support of C.W. are gratefully acknowledged.

IC0520566